



AALBORG UNIVERSITY
DENMARK

Aalborg Universitet

Application of lumped-parameter models

Ibsen, Lars Bo; Liingaard, Morten

Publication date:
2006

Document Version
Publisher's PDF, also known as Version of record

[Link to publication from Aalborg University](#)

Citation for published version (APA):
Ibsen, L. B., & Liingaard, M. (2006). Application of lumped-parameter models. Aalborg: Department of Civil Engineering, Aalborg University. (DCE Technical Reports; No. 12).

General rights

Copyright and moral rights for the publications made accessible in the public portal are retained by the authors and/or other copyright owners and it is a condition of accessing publications that users recognise and abide by the legal requirements associated with these rights.

- ? Users may download and print one copy of any publication from the public portal for the purpose of private study or research.
- ? You may not further distribute the material or use it for any profit-making activity or commercial gain
- ? You may freely distribute the URL identifying the publication in the public portal ?

Take down policy

If you believe that this document breaches copyright please contact us at vbn@aub.aau.dk providing details, and we will remove access to the work immediately and investigate your claim.

Application of lumped-parameter models

Lars Bo Ibsen
Morten Liingaard

Aalborg University
Department of Civil Engineering
Division of Water and Soil

DCE Technical Report No. 12

Application of lumped-parameter models

by

Lars Bo Ibsen
Morten Liingaard

December 2006

© Aalborg University

Scientific Publications at the Department of Civil Engineering

Technical Reports are published for timely dissemination of research results and scientific work carried out at the Department of Civil Engineering (DCE) at Aalborg University. This medium allows publication of more detailed explanations and results than typically allowed in scientific journals.

Technical Memoranda are produced to enable the preliminary dissemination of scientific work by the personnel of the DCE where such release is deemed to be appropriate. Documents of this kind may be incomplete or temporary versions of papers—or part of continuing work. This should be kept in mind when references are given to publications of this kind.

Contract Reports are produced to report scientific work carried out under contract. Publications of this kind contain confidential matter and are reserved for the sponsors and the DCE. Therefore, Contract Reports are generally not available for public circulation.

Lecture Notes contain material produced by the lecturers at the DCE for educational purposes. This may be scientific notes, lecture books, example problems or manuals for laboratory work, or computer programs developed at the DCE.

Theses are monographs or collections of papers published to report the scientific work carried out at the DCE to obtain a degree as either PhD or Doctor of Technology. The thesis is publicly available after the defence of the degree.

Latest News is published to enable rapid communication of information about scientific work carried out at the DCE. This includes the status of research projects, developments in the laboratories, information about collaborative work and recent research results.

Published 2006 by
Aalborg University
Department of Civil Engineering
Sohngaardsholmsvej 57,
DK-9000 Aalborg, Denmark

Printed in Denmark at Aalborg University

ISSN 1901-726X
DCE Technical Report No. 12

Preface

The technical report “Application of lumped-parameter models” is divided into three numbered sections, and a list of references is situated after the last section. Tables, equations and figures are indicated with consecutive numbers. Cited references are marked as e.g. Petyt (1998), with author specification and year of publication in the text.

The work within this report has only been possible with the financial support from the Energy Research Programme (ERP)¹ administered by the Danish Energy Authority. The project is associated with the ERP programme “Soil–Structure interaction of Foundations for Offshore Wind Turbines”. The funding is sincerely acknowledged.

Aalborg, December 11, 2006

Lars Bo Ibsen & Morten Liingaard

¹In danish: “Energiforskningsprogrammet (EFP)”

Contents

1	Application of lumped-parameter models	1
1.1	Lumped-parameter models for the suction caisson	1
1.1.1	Determination of the exact solution for the dynamic stiffness	1
1.1.2	Lumped-parameter models for vertical vibrations	4
1.1.3	Lumped-parameter models for sliding vibrations	8
1.1.4	Lumped-parameter models for rocking vibrations	12
1.1.5	Lumped-parameter models for the coupling term	15
1.1.6	Lumped-parameter models for the torsional term	18
1.2	Assembly of the global dynamic stiffness matrix	21
1.2.1	Structure of the local dynamic stiffness matrices	21
1.2.2	Structure of the global dynamic stiffness matrices	21
1.3	Direct analysis of the steady state response for lumped-parameter models	25
	References	26

List of Figures

1.1	Geometry (a) and BE/FE model (b) of the suction caisson.	2
1.2	Sliding impedance: variation of soil stiffness. $\nu_s = 0.25$ and $\eta_s = 5\%$	3
1.3	Vertical impedance: Boundary element solution and the corresponding lumped-parameter approximation. $\nu_s = 0.25$ and $\eta_s = 5\%$	7
1.4	Sliding impedance: Boundary element solution and the corresponding lumped-parameter approximation. $\nu_s = 0.25$ and $\eta_s = 5\%$	11
1.5	Rocking impedance: Boundary element solution and the corresponding lumped-parameter approximation. $\nu_s = 0.25$ and $\eta_s = 5\%$	14
1.6	Coupling impedance: Boundary element solution and the corresponding lumped-parameter approximation. $\nu_s = 0.25$ and $\eta_s = 5\%$	17
1.7	Torsional impedance: Boundary element solution and the corresponding lumped-parameter approximation. $\nu_s = 0.25$ and $\eta_s = 5\%$	20
1.8	Assembly between global foundation matrices and the structural system.	23
1.9	Structure of the matrices and vectors for the direct analysis.	25

List of Tables

1.1	Model properties for the BE/FE analyses	2
1.2	Vertical: Type and numbers of internal degrees of freedom for the lumped-parameter models	4
1.3	Vertical: Poles and residues	4
1.4	Vertical: Model coefficients	6
1.5	Sliding: Type and numbers of internal degrees of freedom for the lumped-parameter models	8
1.6	Sliding: Poles and residues	8
1.7	Sliding: Model coefficients	10
1.8	Rocking: Type and numbers of internal degrees of freedom for the lumped-parameter models	12
1.9	Rocking: Poles and residues	12
1.10	Rocking: Model coefficients	13
1.11	Coupling: Type and numbers of internal degrees of freedom for the lumped-parameter models	15
1.12	Coupling: Poles and residues	15
1.13	Coupling: Model coefficients	16
1.14	Torsion: Type and numbers of internal degrees of freedom for the lumped-parameter models	18
1.15	Torsion: Poles and residues	18
1.16	Torsion: Model coefficients	19

Chapter 1

Application of lumped-parameter models

This technical report concerns the lumped-parameter models for a suction caisson with a ratio between skirt length and foundation diameter equal to $1/2$, embedded into an viscoelastic soil. The models are presented for three different values of the shear modulus of the subsoil (section 1.1). Subsequently, the assembly of the dynamic stiffness matrix for the foundation is considered (section 1.2), and the solution for obtaining the steady state response, when using lumped-parameter models is given (section 1.2).

1.1 Lumped-parameter models for the suction caisson

The lumped-parameter models have been constructed according to the procedure in Ibsen and Liingaard (2006c). After a brief summary of the modelling procedure for determining the exact solution, the lumped-parameter models for each degree of freedom are given.

1.1.1 Determination of the exact solution for the dynamic stiffness

The frequency dependent dynamic stiffness coefficients are determined by means of a dynamic three-dimensional coupled Boundary Element/Finite Element (BE/FE) program BEASTS by Andersen and Jones (2001). The evaluation of the impedance of suction caisson foundations for offshore wind turbines have been reported in details in Ibsen and Liingaard (2006b) and Ibsen and Liingaard (2006a).

The BE/FE model of the suction caisson consists of four sections: a massless finite element section that forms the top of the foundation where the load is applied, a finite element section of the skirts, a boundary element domain inside the skirts and, finally, a boundary element domain outside the skirts that also forms the free surface. Again, quadratic interpolation is employed. The models of the suction caisson and the subsoil contain approx. 100 finite elements and 350 boundary elements. The mesh of the free surface is truncated at a distance of 30 m (6 times radius R) from the centre of the foundation. The model is illustrated in Figure 1.1. The properties of the soil and the suction caisson used in the BE/FE analyses are given in Table 1.1. Note that ρ_f of the lid of the caisson foundation is zero and that $\rho_f = \rho_s$ for the skirt, in order to model a massless foundation.

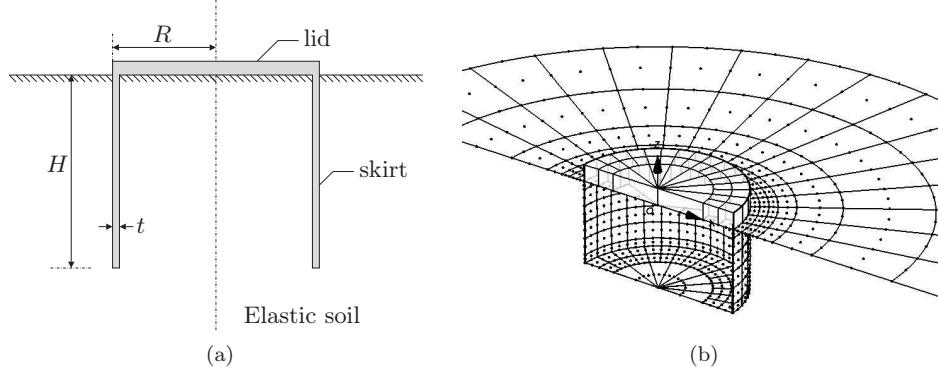


Figure 1.1: Geometry (a) and BE/FE model (b) of the suction caisson.

The dynamic behaviour of the caisson is influenced by ratio between the stiffness of the soil and the stiffness of the structure, see Ibsen and Liingaard (2006b). For low values of G_s the influence of the skirt flexibility vanishes, i.e. the caisson reacts as a rigid foundation. Rigid behaviour can be assumed for $G_s \leq 1.0$ MPa (E_f is constant). On the other hand, the dynamic behaviour of the suction caisson tends towards the frequency dependent behaviour of the surface foundation for high values of G_s (1000 MPa). To show the effects of G_s on the dynamic behaviour of the caisson, the sliding (horizontal) impedance for three values of G_s is shown in Figure 1.2. Note that the impedance changes as the shear modulus of the soil G_s increases. The impedance for $G_s = 1$ MPa and $G_s = 10$ MPa corresponds to that of a rigid suction caisson where the influence of the skirt flexibility vanishes. In contrast, the impedance for $G_s = 100$ MPa corresponds more or less to the behaviour of a surface footing.

Table 1.1: Model properties for the BE/FE analyses

Property		value
Foundation radius	R	6 m
Skirt length	H	6 m
Skirt thickness	t	30 mm
Shear modulus (soil) [†]	G_s	1,10,100 MPa
Poisson's ratio (soil)	ν_s	0.25
Mass density (soil)	ρ_s	1000 kg/m ³
Loss factor (soil)	η_s	5 %
Young's modulus (foundation)	E_f	210 GPa
Poisson's ratio (foundation)	ν_f	0.25
Mass density (foundation) [‡]	ρ_f	0/1000 kg/m ³
Loss factor (foundation)	η_f	2 %

[†] The models are constructed for three values of G_s

[‡] $\rho_f = 0$ for the lid of the caisson and $\rho_f = \rho_s$ for the skirt

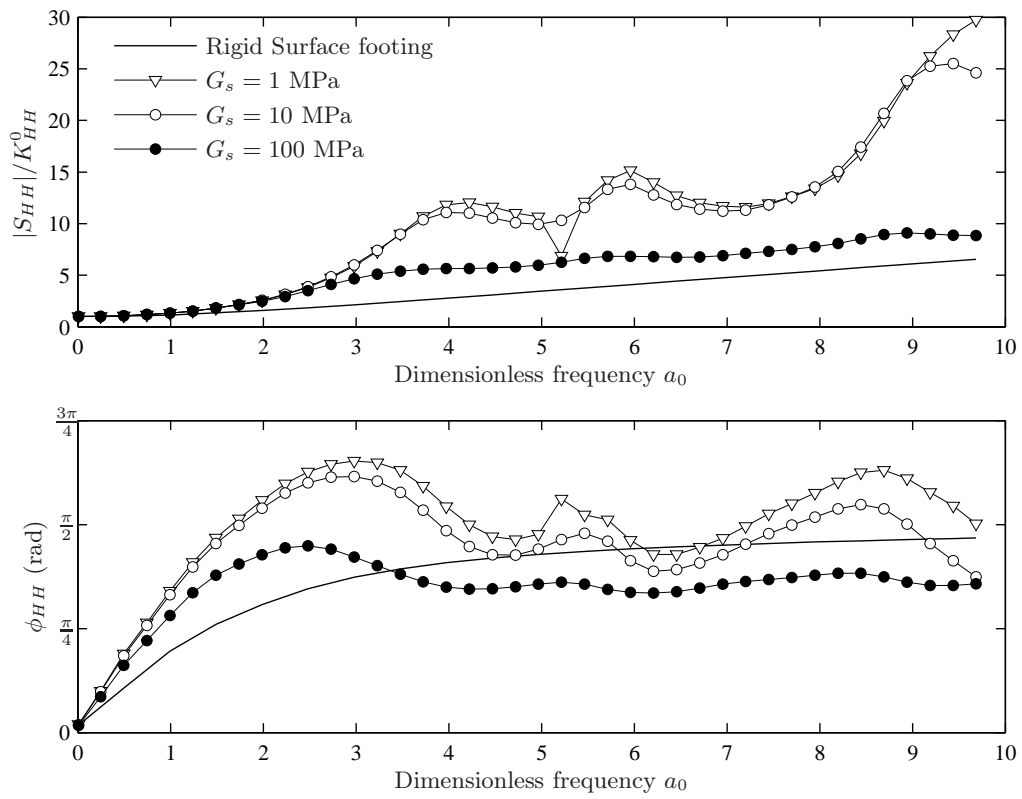


Figure 1.2: Sliding impedance: variation of soil stiffness. $\nu_s = 0.25$ and $\eta_s = 5\%$.

Table 1.2: Vertical: Type and numbers of internal degrees of freedom for the lumped-parameter models

G_s	Type	No. of internal dofs
1.0	3 second-order (kcm [†])	3
10	2 second-order (kcm [†]) + 1 first-order (kcm [‡])	3
100	2 second-order (kcm [†]) + 1 first-order (kcm [‡])	3

[†] Spring-dashpot-mass model, see Figure 1.10b in Ibsen and Liingaard (2006c)
[‡] Spring-dashpot-mass model, see Figure 1.9b in Ibsen and Liingaard (2006c)

1.1.2 Lumped-parameter models for vertical vibrations

The type of approximation for the vertical lumped-parameter models is summarized in Table 1.2 and the approximation is compared with the rigorous solution in Figure 1.3. The pole-residue coefficients, the stiffness, damping and mass matrices of the models are given in the following.

Pole-residue coefficients

Table 1.3: Vertical: Poles and residues

	Poles s	Residues A
$G_s = 1$ MPa	$-3.6431 + 5.0238i$	$-5.7562 - 25.4628i$
	$-3.6431 - 5.0238i$	$-5.7562 + 25.4628i$
	$-1.2197 + 2.8101i$	$-2.5259 + 3.6613i$
	$-1.2197 - 2.8101i$	$-2.5259 - 3.6613i$
	$-0.5940 + 0.9980i$	$-0.3678 + 5.1392i$
	$-0.5940 - 0.9980i$	$-0.3678 - 5.1392i$
$G_s = 10$ MPa	-2.5113	$+0.5776$
	$-0.8520 + 4.5455i$	$-1.1955 - 2.3842i$
	$-0.8520 - 4.5455i$	$-1.1955 + 2.3842i$
	$-0.7600 + 2.2086i$	$-1.1895 - 0.2391i$
	$-0.7600 - 2.2086i$	$-1.1895 + 0.2391i$
$G_s = 100$ MPa	-23.8012	$+89.6892$
	$-1.1905 + 2.2720i$	$-0.4714 + 2.8058i$
	$-1.1905 - 2.2720i$	$-0.4714 - 2.8058i$
	$-0.9607 + 4.7741i$	$+0.4145 + 1.7268i$
	$-0.9607 - 4.7741i$	$+0.4145 - 1.7268i$

Matrices for the models

The resulting matrices of the models are given by Equations 1.1 and 1.2. The model structure stated in Equation 1.1 corresponds to the lumped-parameter model with three complex conjugate poles ($G_s = 1$ MPa), whereas the model structure stated in Equation 1.2 corresponds to the lumped-parameter models with one real and two complex conjugate poles ($G_s = 10$ MPa and 100 MPa). The corresponding coefficients are listed in Table 1.4.

$$\mathbf{K}_{\mathbf{V}\mathbf{V}} = K_{VV}^0 \begin{bmatrix} \frac{\gamma_1^2}{\mu_1} + \frac{\gamma_2^2}{\mu_2} + \frac{\gamma_3^2}{\mu_3} & -\kappa_1 & -\kappa_3 & -\kappa_5 \\ -\kappa_1 & \kappa_1 + \kappa_2 & 0 & 0 \\ -\kappa_3 & 0 & \kappa_3 + \kappa_4 & 0 \\ -\kappa_5 & 0 & 0 & \kappa_5 + \kappa_6 \end{bmatrix} \quad (1.1a)$$

$$\mathbf{C}_{\mathbf{V}\mathbf{V}} = \frac{R}{c_S} K_{VV}^0 \begin{bmatrix} c^\infty & -\gamma_1 & -\gamma_2 & -\gamma_3 \\ -\gamma_1 & 2\gamma_1 & 0 & 0 \\ -\gamma_2 & 0 & 2\gamma_2 & 0 \\ -\gamma_3 & 0 & 0 & 2\gamma_3 \end{bmatrix} \quad (1.1b)$$

$$\mathbf{M}_{\mathbf{V}\mathbf{V}} = \frac{R^2}{c_S^2} K_{VV}^0 \begin{bmatrix} 0 & 0 & 0 & 0 \\ 0 & \mu_1 & 0 & 0 \\ 0 & 0 & \mu_2 & 0 \\ 0 & 0 & 0 & \mu_3 \end{bmatrix} \quad (1.1c)$$

$$\mathbf{K}_{\mathbf{V}\mathbf{V}} = K_{VV}^0 \begin{bmatrix} \frac{\gamma_1^2}{\mu_1} + \frac{\gamma_2^2}{\mu_2} + \frac{\gamma_3^2}{\mu_3} & -\kappa_1 & -\kappa_3 & 0 \\ -\kappa_1 & \kappa_1 + \kappa_2 & 0 & 0 \\ -\kappa_3 & 0 & \kappa_3 + \kappa_4 & 0 \\ 0 & 0 & 0 & 0 \end{bmatrix} \quad (1.2a)$$

$$\mathbf{C}_{\mathbf{V}\mathbf{V}} = \frac{R}{c_S} K_{VV}^0 \begin{bmatrix} c^\infty & -\gamma_1 & -\gamma_2 & -\gamma_3 \\ -\gamma_1 & 2\gamma_1 & 0 & 0 \\ -\gamma_2 & 0 & 2\gamma_2 & 0 \\ -\gamma_3 & 0 & 0 & \gamma_3 \end{bmatrix} \quad (1.2b)$$

$$\mathbf{M}_{\mathbf{V}\mathbf{V}} = \frac{R^2}{c_S^2} K_{VV}^0 \begin{bmatrix} 0 & 0 & 0 & 0 \\ 0 & \mu_1 & 0 & 0 \\ 0 & 0 & \mu_2 & 0 \\ 0 & 0 & 0 & \mu_3 \end{bmatrix} \quad (1.2c)$$

Note that the limiting damping parameter for $G_s = 100$ MPa has been fitted manually. Since the impedance for high values of G_s approaches the frequency dependent behaviour of the surface footings, the solution in Ibsen and Liingaard (2006b) is not valid. c^∞ for $G_s = 100$ MPa in Table 1.4 is in between the value for the suction caisson and a surface footing.

Table 1.4: Vertical: Model coefficients

	κ coeff.	Value	γ coeff.	Value	μ coeff.	Value	misc	Value
$G_s = 1$ MPa	κ_1	11.8449	γ_1	2.8176	μ_1	0.7734	c^∞	2.2581
	κ_2	17.9400	γ_2	0.0037	μ_2	0.0062	K_{VV}^0	7.9747
	κ_3	0.6215	γ_3	0.2296	μ_3	0.1882		
	κ_4	-0.3958						
	κ_5	2.3510						
	κ_6	-0.5848						
$G_s = 10$ MPa	κ_1	2.5145	γ_1	1.3043	μ_1	1.5309	c^∞	2.3107
	κ_2	30.2269	γ_2	0.8653	μ_2	1.1385	K_{VV}^0	7.7933
	κ_3	2.2228	γ_3	0.0916	μ_3	0.0365		
	κ_4	3.9882						
$G_s = 100$ MPa	κ_1	-0.4212	γ_1	0.0107	μ_1	0.0111	c^∞	0.4208 [†]
	κ_2	0.6852	γ_2	0.0145	μ_2	0.0122	K_{VV}^0	6.4658
	κ_3	0.4132	γ_3	0.1583	μ_3	0.0067		
	κ_4	-0.3329						

[†] Manual fit.

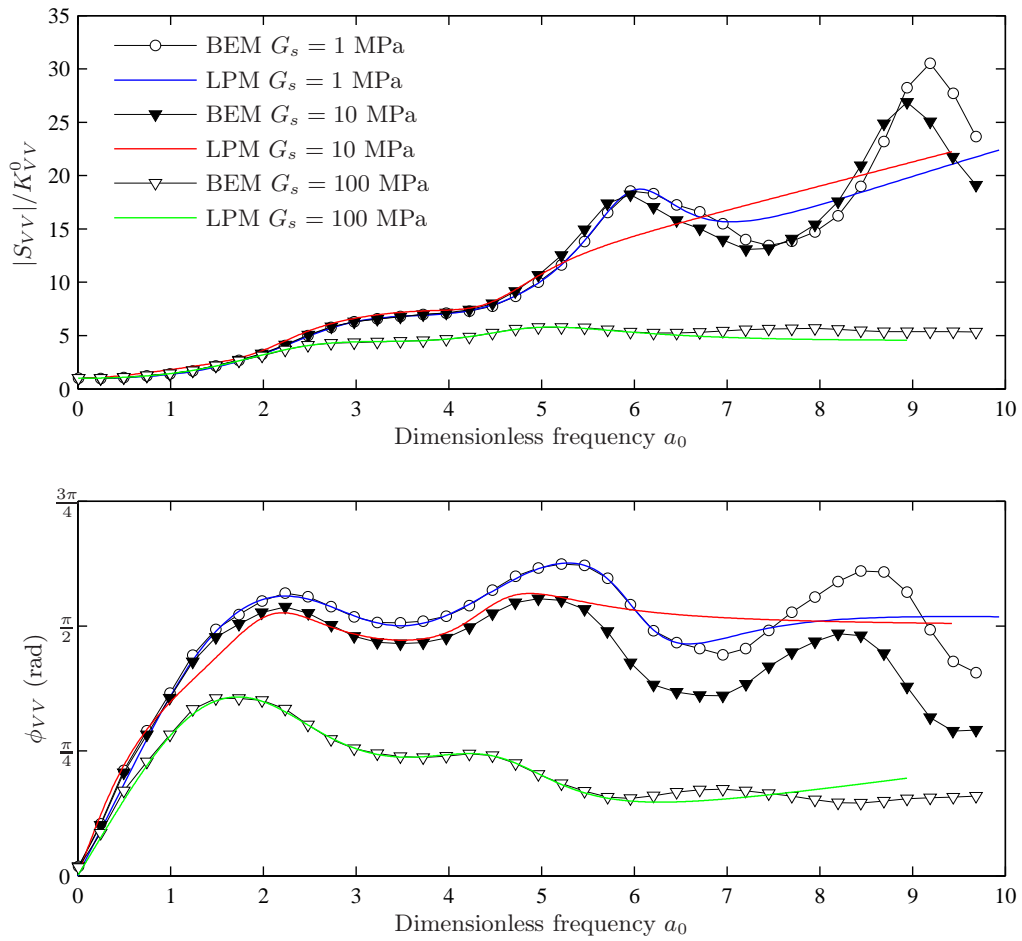


Figure 1.3: Vertical impedance: Boundary element solution and the corresponding lumped-parameter approximation. $\nu_s = 0.25$ and $\eta_s = 5\%$.

Table 1.5: Sliding: Type and numbers of internal degrees of freedom for the lumped-parameter models

G_s	Type	No. of internal dofs
1.0	3 second-order (kcm [†])	3
10	3 second-order (kcm [†])	3
100	2 second-order (kcm [†]) + 1 first-order (kcm [‡])	3

[†] Spring-dashpot-mass model, see Figure 1.10b in Ibsen and Liingaard (2006c)
[‡] Spring-dashpot-mass model, see Figure 1.9b in Ibsen and Liingaard (2006c)

1.1.3 Lumped-parameter models for sliding vibrations

The type of approximation for the horizontal lumped-parameter models is summarized in Table 1.5 and the approximation is compared with the rigorous solution in Figure 1.4. The pole-residue coefficients, the stiffness, damping and mass matrices of the models are given in the following.

Pole-residue coefficients

Table 1.6: Sliding: Poles and residues

	Poles s	Residues A
$G_s = 1$ MPa	$-3.1835 + 4.8983i$	$-14.2305 - 32.9079i$
	$-3.1835 - 4.8983i$	$-14.2305 + 32.9079i$
	$-0.5497 + 5.7479i$	$-1.6722 + 4.9951i$
	$-0.5497 - 5.7479i$	$-1.6722 - 4.9951i$
	$-1.0329 + 4.4915i$	$+7.9207 + 11.3350i$
	$-1.0329 - 4.4915i$	$+7.9207 - 11.3350i$
$G_s = 10$ MPa	$-2.9289 + 7.0308i$	$-6.6629 - 23.0006i$
	$-2.9289 - 7.0308i$	$-6.6629 + 23.0006i$
	$-0.5447 + 5.7685i$	$-0.8154 + 3.0212i$
	$-0.5447 - 5.7685i$	$-0.8154 - 3.0212i$
	$-0.8437 + 3.7649i$	$-2.4717 + 4.9915i$
	$-0.8437 - 3.7649i$	$-2.4717 - 4.9915i$
$G_s = 100$ MPa	-14.9506	$+45.7048$
	$-0.6453 + 5.5078i$	$-0.0784 + 0.6483i$
	$-0.6453 - 5.5078i$	$-0.0784 - 0.6483i$
	$-1.2456 + 3.0948i$	$-0.9869 + 2.9066i$
	$-1.2456 - 3.0948i$	$-0.9869 - 2.9066i$

Matrices for the models

The resulting matrices of the models are given by Equations 1.3 and 1.4. The model structure stated in Equation 1.3 corresponds to the lumped-parameter model with three complex conjugate poles ($G_s = 1$ and 10 MPa), whereas the model structure stated in Equation 1.4 corresponds to the lumped-parameter model with one real and two complex conjugate poles ($G_s = 100$ MPa). The corresponding coefficients are listed in Table 1.7.

$$\mathbf{K}_{\text{HH}} = K_{\text{HH}}^0 \begin{bmatrix} \frac{\gamma_1^2}{\mu_1} + \frac{\gamma_2^2}{\mu_2} + \frac{\gamma_3^2}{\mu_3} & -\kappa_1 & -\kappa_3 & -\kappa_5 \\ -\kappa_1 & \kappa_1 + \kappa_2 & 0 & 0 \\ -\kappa_3 & 0 & \kappa_3 + \kappa_4 & 0 \\ -\kappa_5 & 0 & 0 & \kappa_5 + \kappa_6 \end{bmatrix} \quad (1.3a)$$

$$\mathbf{C}_{\text{HH}} = \frac{R}{c_S} K_{\text{HH}}^0 \begin{bmatrix} c^\infty & -\gamma_1 & -\gamma_2 & -\gamma_3 \\ -\gamma_1 & 2\gamma_1 & 0 & 0 \\ -\gamma_2 & 0 & 2\gamma_2 & 0 \\ -\gamma_3 & 0 & 0 & 2\gamma_3 \end{bmatrix} \quad (1.3b)$$

$$\mathbf{M}_{\text{HH}} = \frac{R^2}{c_S^2} K_{\text{HH}}^0 \begin{bmatrix} 0 & 0 & 0 & 0 \\ 0 & \mu_1 & 0 & 0 \\ 0 & 0 & \mu_2 & 0 \\ 0 & 0 & 0 & \mu_3 \end{bmatrix} \quad (1.3c)$$

$$\mathbf{K}_{\text{HH}} = K_{\text{HH}}^0 \begin{bmatrix} \frac{\gamma_1^2}{\mu_1} + \frac{\gamma_2^2}{\mu_2} + \frac{\gamma_3^2}{\mu_3} & -\kappa_1 & -\kappa_3 & 0 \\ -\kappa_1 & \kappa_1 + \kappa_2 & 0 & 0 \\ -\kappa_3 & 0 & \kappa_3 + \kappa_4 & 0 \\ 0 & 0 & 0 & 0 \end{bmatrix} \quad (1.4a)$$

$$\mathbf{C}_{\text{HH}} = \frac{R}{c_S} K_{\text{HH}}^0 \begin{bmatrix} c^\infty & -\gamma_1 & -\gamma_2 & -\gamma_3 \\ -\gamma_1 & 2\gamma_1 & 0 & 0 \\ -\gamma_2 & 0 & 2\gamma_2 & 0 \\ -\gamma_3 & 0 & 0 & \gamma_3 \end{bmatrix} \quad (1.4b)$$

$$\mathbf{M}_{\text{HH}} = \frac{R^2}{c_S^2} K_{\text{HH}}^0 \begin{bmatrix} 0 & 0 & 0 & 0 \\ 0 & \mu_1 & 0 & 0 \\ 0 & 0 & \mu_2 & 0 \\ 0 & 0 & 0 & \mu_3 \end{bmatrix} \quad (1.4c)$$

Note that the limiting damping parameter for $G_s = 100$ MPa has been fitted manually. Since the impedance for high values of G_s approaches the frequency dependent behaviour of the surface footings, the solution in Ibsen and Liingaard (2006a) is not valid. c^∞ for $G_s = 100$ MPa in Table 1.7 is in between the value for the suction caisson and a surface footing.

Table 1.7: Sliding: Model coefficients

	κ coeff.	Value	γ coeff.	Value	μ coeff.	Value	misc	Value
$G_s = 1$ MPa	κ_1	18.5077	γ_1	4.4095	μ_1	1.3851	c^∞	2.1480
	κ_2	28.7646	γ_2	0.0862	μ_2	0.1569	K_{HH}^0	9.4540
	κ_3	3.0895	γ_3	0.5374	μ_3	0.5203		
	κ_4	2.1411						
	κ_5	-7.1135						
	κ_6	18.1655						
$G_s = 10$ MPa	κ_1	8.9522	γ_1	2.2798	μ_1	0.7784	c^∞	2.2035
	κ_2	36.2012	γ_2	0.0344	μ_2	0.0631	K_{HH}^0	9.2162
	κ_3	1.5156	γ_3	0.1821	μ_3	0.2158		
	κ_4	0.6045						
	κ_5	3.0832						
	κ_6	0.1297						
$G_s = 100$ MPa	κ_1	0.1224	γ_1	0.0013	μ_1	0.0021	c^∞	0.9275 [†]
	κ_2	-0.0590	γ_2	0.0423	μ_2	0.0339	K_{HH}^0	7.8288
	κ_3	0.8450	γ_3	0.2045	μ_3	0.0137		
	κ_4	-0.4672						

[†] Manual fit.

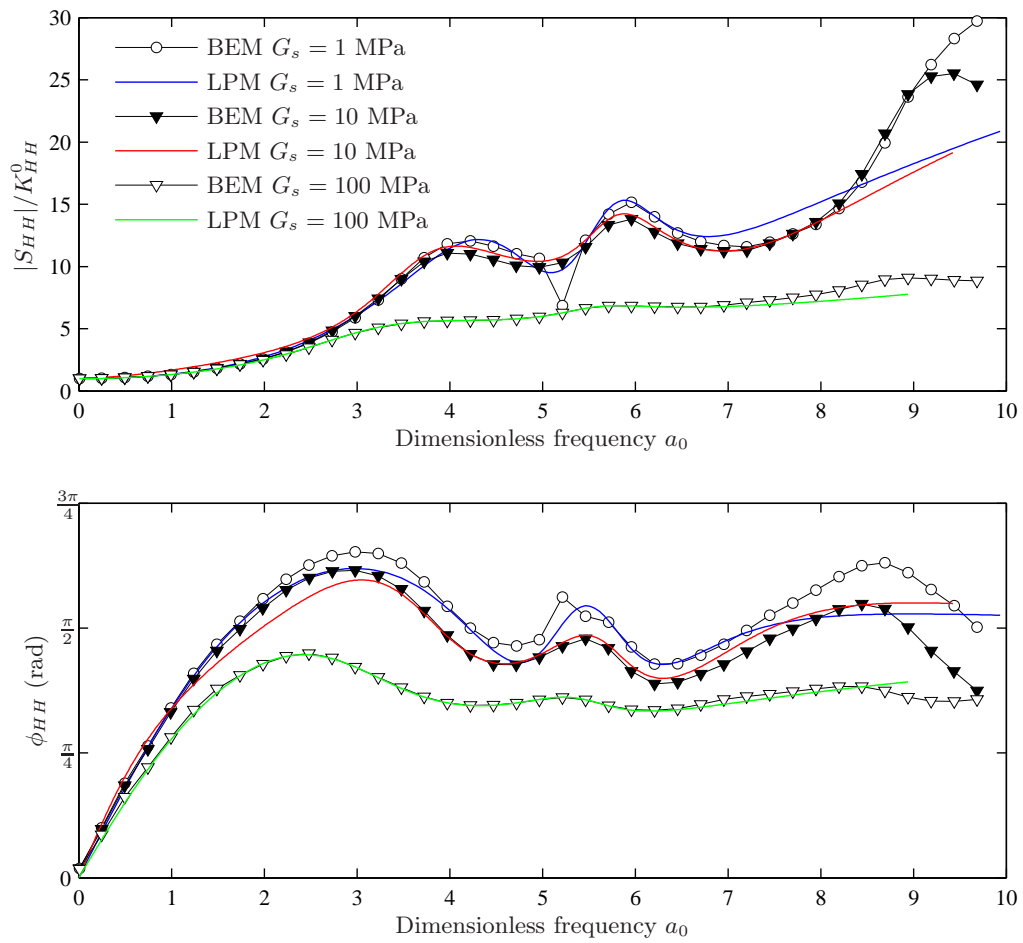


Figure 1.4: Sliding impedance: Boundary element solution and the corresponding lumped-parameter approximation. $\nu_s = 0.25$ and $\eta_s = 5\%$.

Table 1.8: Rocking: Type and numbers of internal degrees of freedom for the lumped-parameter models

G_s	Type	No. of internal dofs
1.0	2 second-order (kcm [†]) + 1 first-order (kcm [‡])	3
10	2 second-order (kcm [†]) + 1 first-order (kcm [‡])	3
100	2 second-order (kcm [†]) + 1 first-order (kcm [‡])	3

[†] Spring-dashpot-mass model, see Figure 1.10b in Ibsen and Liingaard (2006c)
[‡] Spring-dashpot-mass model, see Figure 1.9b in Ibsen and Liingaard (2006c)

1.1.4 Lumped-parameter models for rocking vibrations

The type of approximation for the rocking lumped-parameter models is summarized in Table 1.8 and the approximation is compared with the rigorous solution in Figure 1.5. The pole-residue coefficients, the stiffness, damping and mass matrices of the models are given in the following.

Pole-residue coefficients

Table 1.9: Rocking: Poles and residues

	Poles s	Residues A
$G_s = 1$ MPa	-2.2574	3.0119
	-0.4660 + 4.2593i	+0.2815 + 0.9699i
	-0.4660 - 4.2593i	+0.2815 - 0.9699i
	-0.2503 + 6.2918i	+0.0514 - 0.2789i
	-0.2503 - 6.2918i	+0.0514 + 0.2789i
$G_s = 10$ MPa	-8.2898 + 5.8728i	-11.3577 - 30.0471i
	-8.2898 - 5.8728i	-11.3577 + 30.0471i
	-0.9062	+0.1849
	-0.7761 + 4.2620i	+0.8639 + 1.9198i
	-0.7761 - 4.2620i	+0.8639 - 1.9198i
$G_s = 100$ MPa	-21.2318	+30.5256
	-2.2326 + 0.4371i	-1.2139 - 4.1473i
	-2.2326 - 0.4371i	-1.2139 + 4.1473i
	-0.6393 + 4.3133i	+0.4135 + 0.2652i
	-0.6393 - 4.3133i	+0.4135 - 0.2652i

Matrices for the models

The resulting matrices of the models are given by Equation 1.5. The model structure stated in Equation 1.5 corresponds to the lumped-parameter models with one real and two complex conjugate poles. The corresponding coefficients are listed in Table 1.10.

$$\mathbf{K}_{\text{MM}} = K_{\text{MM}}^0 \begin{bmatrix} \frac{\gamma_1^2}{\mu_1} + \frac{\gamma_2^2}{\mu_2} + \frac{\gamma_3^2}{\mu_3} & -\kappa_1 & -\kappa_3 & 0 \\ -\kappa_1 & \kappa_1 + \kappa_2 & 0 & 0 \\ -\kappa_3 & 0 & \kappa_3 + \kappa_4 & 0 \\ 0 & 0 & 0 & 0 \end{bmatrix} \quad (1.5a)$$

$$\mathbf{C}_{\text{MM}} = \frac{R}{c_S} K_{\text{MM}}^0 \begin{bmatrix} c^\infty & -\gamma_1 & -\gamma_2 & -\gamma_3 \\ -\gamma_1 & 2\gamma_1 & 0 & 0 \\ -\gamma_2 & 0 & 2\gamma_2 & 0 \\ -\gamma_3 & 0 & 0 & \gamma_3 \end{bmatrix} \quad (1.5b)$$

$$\mathbf{M}_{\text{MM}} = \frac{R^2}{c_S^2} K_{\text{MM}}^0 \begin{bmatrix} 0 & 0 & 0 & 0 \\ 0 & \mu_1 & 0 & 0 \\ 0 & 0 & \mu_2 & 0 \\ 0 & 0 & 0 & \mu_3 \end{bmatrix} \quad (1.5c)$$

Table 1.10: Rocking: Model coefficients

	κ coeff.	Value	γ coeff.	Value	μ coeff.	Value	misc	Value
$G_s = 1$ MPa	κ_1	-0.1161	γ_1	0.3572	μ_1	1.4275	c^∞	0.8055
	κ_2	56.7137	γ_2	0.0202	μ_2	0.0433	K_{MM}^0	16.5930
	κ_3	-0.5946	γ_3	0.5910	μ_3	0.2618		
	κ_4	1.3887						
$G_s = 10$ MPa	κ_1	11.9561	γ_1	1.2770	μ_1	0.1540	c^∞	0.8415
	κ_2	3.9427	γ_2	0.0561	μ_2	0.0722	K_{MM}^0	15.8830
	κ_3	-1.0696	γ_3	0.2252	μ_3	0.2485		
	κ_4	2.4251						
$G_s = 100$ MPa	κ_1	-0.5945	γ_1	0.0820	μ_1	0.1283	c^∞	0.3959 [†]
	κ_2	3.033	γ_2	8.6772	μ_2	3.8865	K_{MM}^0	11.8941
	κ_3	19.9167	γ_3	0.0677	μ_3	0.0032		
	κ_4	0.1989						

[†] Manual fit.

Note that the limiting damping parameter for $G_s = 100$ MPa has been fitted manually. Since the impedance for high values of G_s approaches the frequency dependent behaviour of the surface footings, the solution in Ibsen and Liingaard (2006a) is not valid. c^∞ for $G_s = 100$ MPa in Table 1.10 is in between the value for the suction caisson and a surface footing.

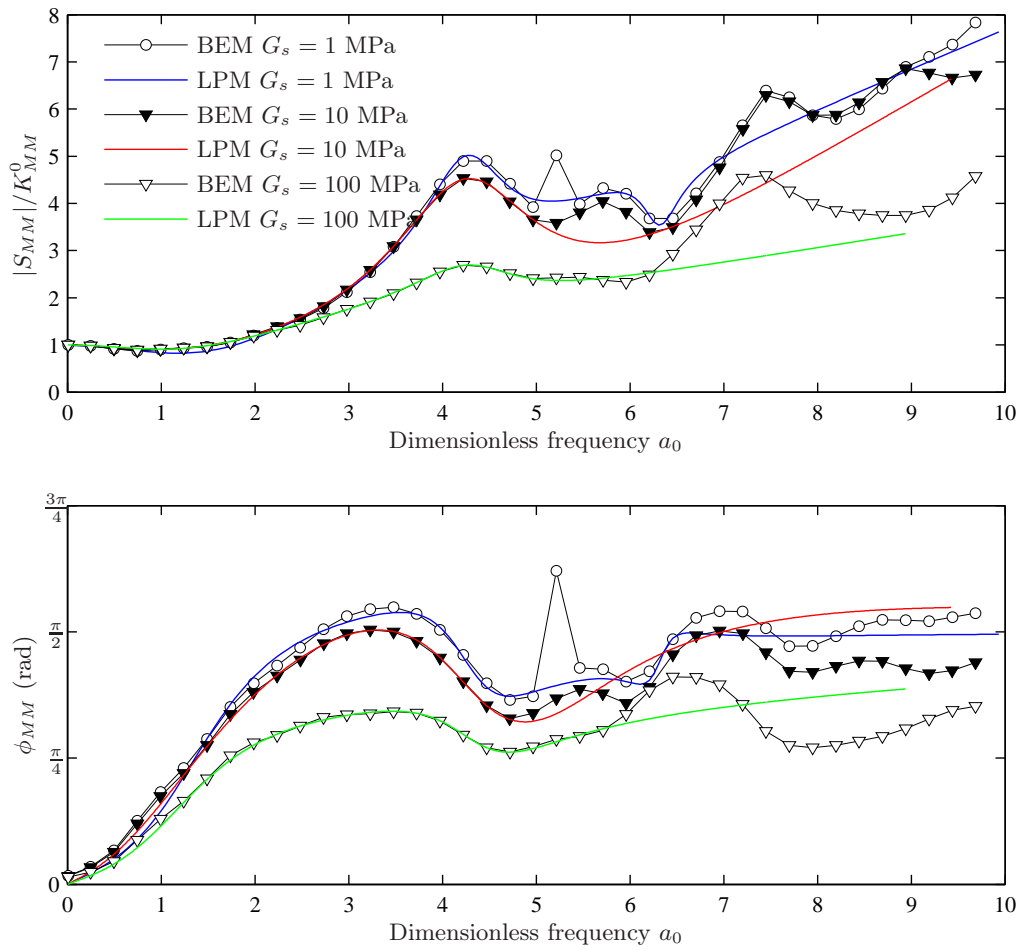


Figure 1.5: Rocking impedance: Boundary element solution and the corresponding lumped-parameter approximation. $\nu_s = 0.25$ and $\eta_s = 5\%$.

Table 1.11: Coupling: Type and numbers of internal degrees of freedom for the lumped-parameter models

G_s	Type	No. of internal dofs
1.0	2 second-order (kcm [†]) + 1 first-order (kcm [‡])	3
10	2 second-order (kcm [†]) + 1 first-order (kcm [‡])	3
100	2 second-order (kcm [†]) + 1 first-order (kcm [‡])	3

[†] Spring-dashpot-mass model, see Figure 1.10b in Ibsen and Liingaard (2006c)
[‡] Spring-dashpot-mass model, see Figure 1.9b in Ibsen and Liingaard (2006c)

1.1.5 Lumped-parameter models for the coupling term

The type of approximation for the coupling lumped-parameter models is summarized in Table 1.11 and the approximation is compared with the rigorous solution in Figure 1.6. The pole-residue coefficients, the stiffness, damping and mass matrices of the models are given in the following.

Pole-residue coefficients

Table 1.12: Coupling: Poles and residues

	Poles s	Residues A
$G_s = 1$ MPa	-3.2542	+9.7824
	-0.6757 + 4.2024i	+1.4116 + 3.6383i
	-0.6757 - 4.2024i	+1.4116 - 3.6383i
	-0.3401 + 5.9793i	+1.0812 + 1.3791i
	-0.3401 - 5.9793i	+1.0812 - 1.3791i
$G_s = 10$ MPa	-2.9049	+5.5089
	-0.5912 + 4.1399i	+1.9160 + 2.2139i
	-0.5912 - 4.1399i	+1.9160 - 2.2139i
	-0.4251 + 6.1778i	+2.2902 - 0.0207i
	-0.4251 - 6.1778i	+2.2902 + 0.0207i
$G_s = 100$ MPa	-3.5564 + 8.5065i	+21.7153 + 3.5724i
	-3.5564 - 8.5065i	+21.7153 - 3.5724i
	-1.2170	+0.2659
	-0.9167 + 3.5203i	+2.7409 + 1.3198i
	-0.9167 - 3.5203i	+2.7409 - 1.3198i

Matrices for the models

The resulting matrices of the models are given by Equation 1.6. The model structure stated in Equation 1.6 corresponds to the lumped-parameter models with one real and two complex conjugate poles. The corresponding coefficients are listed in Table 1.13.

$$\mathbf{K}_{\text{HM}} = K_{\text{HM}}^0 \begin{bmatrix} \frac{\gamma_1^2}{\mu_1} + \frac{\gamma_2^2}{\mu_2} + \frac{\gamma_3^2}{\mu_3} & -\kappa_1 & -\kappa_3 & 0 \\ -\kappa_1 & \kappa_1 + \kappa_2 & 0 & 0 \\ -\kappa_3 & 0 & \kappa_3 + \kappa_4 & 0 \\ 0 & 0 & 0 & 0 \end{bmatrix} \quad (1.6a)$$

$$\mathbf{C}_{\text{HM}} = \frac{R}{c_S} K_{\text{HM}}^0 \begin{bmatrix} c^\infty & -\gamma_1 & -\gamma_2 & -\gamma_3 \\ -\gamma_1 & 2\gamma_1 & 0 & 0 \\ -\gamma_2 & 0 & 2\gamma_2 & 0 \\ -\gamma_3 & 0 & 0 & \gamma_3 \end{bmatrix} \quad (1.6b)$$

$$\mathbf{M}_{\text{HM}} = \frac{R^2}{c_S^2} K_{\text{HM}}^0 \begin{bmatrix} 0 & 0 & 0 & 0 \\ 0 & \mu_1 & 0 & 0 \\ 0 & 0 & \mu_2 & 0 \\ 0 & 0 & 0 & \mu_3 \end{bmatrix} \quad (1.6c)$$

$$(1.6d)$$

Table 1.13: Coupling: Model coefficients

	κ coeff.	Value	γ coeff.	Value	μ coeff.	Value	misc	Value
$G_s = 1$ MPa	κ_1	-3.1170	γ_1	0.1836	μ_1	0.5399	c^∞	1.3253
	κ_2	22.4813	γ_2	0.0931	μ_2	0.1377	K_{HM}^0	-6.4765
	κ_3	-2.0263	γ_3	0.9238	μ_3	0.2839		
	κ_4	4.5215						
$G_s = 10$ MPa	κ_1	-5.0128	γ_1	0.8799	μ_1	2.0697	c^∞	1.4061
	κ_2	84.3772	γ_2	0.2917	μ_2	0.4935	K_{HM}^0	-6.1043
	κ_3	-3.0686	γ_3	0.6528	μ_3	0.2247		
	κ_4	11.6986						
$G_s = 100$ MPa	κ_1	-0.4212	γ_1	0.0107	μ_1	0.0111	c^∞	0.4208 [†]
	κ_2	0.6852	γ_2	0.0145	μ_2	0.0122	K_{HM}^0	-4.0359
	κ_3	0.4132	γ_3	0.1583	μ_3	0.0067		
	κ_4	-0.3329						

[†] Manual fit.

Note that the limiting damping parameter for $G_s = 100$ MPa has been fitted manually. Since the impedance for high values of G_s approaches the frequency dependent behaviour of the surface footings, the solution in Ibsen and Liingaard (2006a) is not valid. c^∞ for $G_s = 100$ MPa in Table 1.13 is in between the value for the suction caisson and a surface footing.

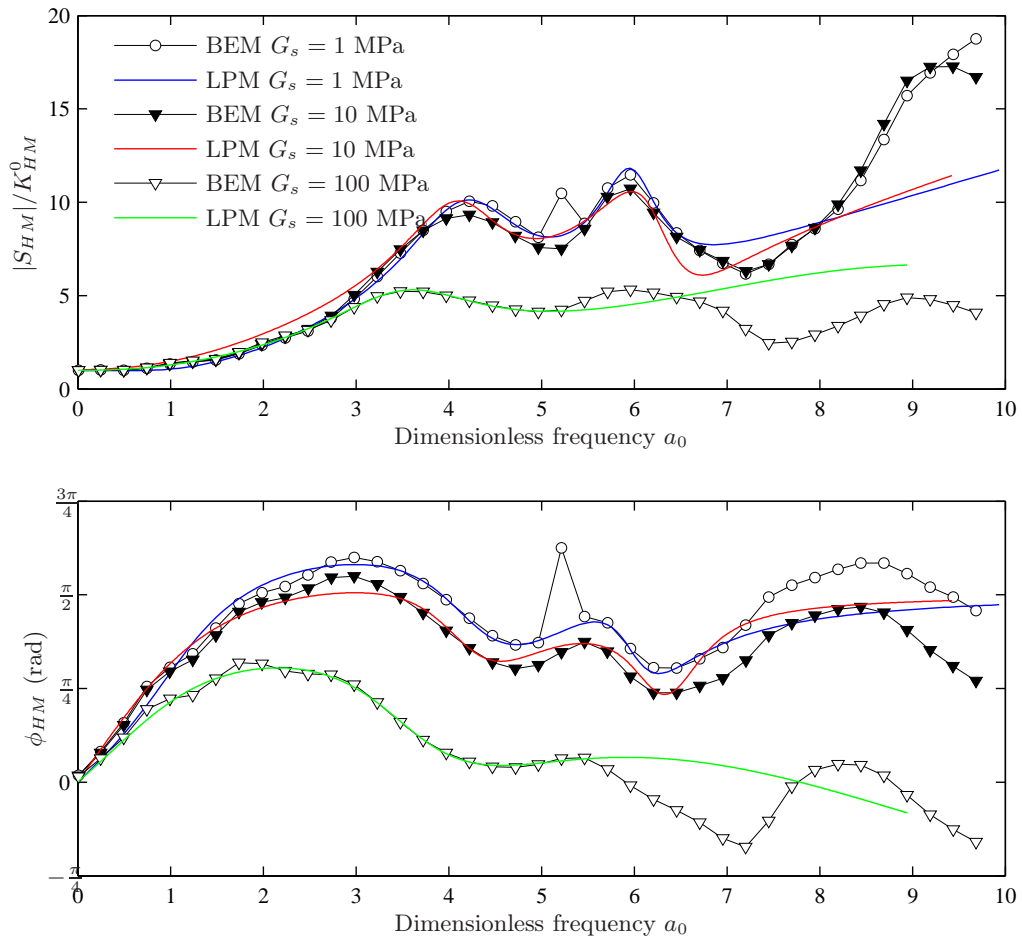


Figure 1.6: Coupling impedance: Boundary element solution and the corresponding lumped-parameter approximation. $\nu_s = 0.25$ and $\eta_s = 5\%$.

Table 1.14: Torsion: Type and numbers of internal degrees of freedom for the lumped-parameter models

G_s	Type	No. of internal dofs
1.0	2 second-order (kcm [†]) + 1 first-order (kcm [‡])	3
10	2 second-order (kcm [†]) + 1 first-order (kcm [‡])	3
100	2 second-order (kcm [†]) + 1 first-order (kcm [‡])	3

[†] Spring-dashpot-mass model, see Figure 1.10b in Ibsen and Liingaard (2006c)
[‡] Spring-dashpot-mass model, see Figure 1.9b in Ibsen and Liingaard (2006c)

1.1.6 Lumped-parameter models for the torsional term

The type of approximation for the torsional lumped-parameter models is summarized in Table 1.14 and the approximation is compared with the rigorous solution in Figure 1.7. The pole-residue coefficients, the stiffness, damping and mass matrices of the models are given in the following.

Pole-residue coefficients

Table 1.15: Torsion: Poles and residues

	Poles s	Residues A
$G_s = 1$ MPa	$-2.0852 + 4.7267i$	$-0.9261 - 3.4940i$
	$-2.0852 - 4.7267i$	$-0.9261 + 3.4940i$
	-1.3704	$+0.8947$
	$-0.5230 + 4.4196i$	$-0.0782 + 1.6683i$
	$-0.5230 - 4.4196i$	$-0.0782 - 1.6683i$
$G_s = 10$ MPa	$-2.8905 + 5.2170i$	$-1.6770 - 4.9680i$
	$-2.8905 - 5.2170i$	$-1.6770 + 4.9680i$
	-1.2508	$+0.6362$
	$-0.5122 + 4.3775i$	$-0.1489 + 1.5255i$
	$-0.5122 - 4.3775i$	$-0.1489 - 1.5255i$
$G_s = 100$ MPa	-4.6430	$+8.7857$
	$-0.6051 + 4.2483i$	$+0.4685 + 1.4270i$
	$-0.6051 - 4.2483i$	$+0.4685 - 1.4270i$
	$-0.4184 + 7.1604i$	$+0.9069 + 1.0041i$
	$-0.4184 - 7.1604i$	$+0.9069 - 1.0041i$

Matrices for the models

The resulting matrices of the models are given by Equation 1.7. The model structure stated in Equation 1.7 corresponds to the lumped-parameter models with one real and two complex conjugate poles. The corresponding coefficients are listed in Table 1.16.

$$\mathbf{K}_{\text{TT}} = K_{TT}^0 \begin{bmatrix} \frac{\gamma_1^2}{\mu_1} + \frac{\gamma_2^2}{\mu_2} + \frac{\gamma_3^2}{\mu_3} & -\kappa_1 & -\kappa_3 & 0 \\ -\kappa_1 & \kappa_1 + \kappa_2 & 0 & 0 \\ -\kappa_3 & 0 & \kappa_3 + \kappa_4 & 0 \\ 0 & 0 & 0 & 0 \end{bmatrix} \quad (1.7a)$$

$$\mathbf{C}_{\text{TT}} = \frac{R}{c_S} K_{TT}^0 \begin{bmatrix} c^\infty & -\gamma_1 & -\gamma_2 & -\gamma_3 \\ -\gamma_1 & 2\gamma_1 & 0 & 0 \\ -\gamma_2 & 0 & 2\gamma_2 & 0 \\ -\gamma_3 & 0 & 0 & \gamma_3 \end{bmatrix} \quad (1.7b)$$

$$\mathbf{M}_{\text{TT}} = \frac{R^2}{c_S^2} K_{TT}^0 \begin{bmatrix} 0 & 0 & 0 & 0 \\ 0 & \mu_1 & 0 & 0 \\ 0 & 0 & \mu_2 & 0 \\ 0 & 0 & 0 & \mu_3 \end{bmatrix} \quad (1.7c)$$

$$(1.7d)$$

Table 1.16: Torsion: Model coefficients

	κ coeff.	Value	γ coeff.	Value	μ coeff.	Value	misc	Value
$G_s = 1$ MPa	κ_1	1.9481	γ_1	0.7212	μ_1	0.3459	c^∞	0.7257
	κ_2	7.2834	γ_2	0.0008	μ_2	0.0015	K_{TT}^0	19.4817
	κ_3	0.1500	γ_3	0.4764	μ_3	0.3477		
	κ_4	-0.1199						
$G_s = 10$ MPa	κ_1	2.5375	γ_1	0.6772	μ_1	0.2343	c^∞	0.7382
	κ_2	5.7962	γ_2	0.0032	μ_2	0.0063	K_{TT}^0	19.1516
	κ_3	0.2923	γ_3	0.4066	μ_3	0.3251		
	κ_4	-0.1697						
$G_s = 100$ MPa	κ_1	-2.1190	γ_1	0.1165	μ_1	0.2784	c^∞	0.5363 [†]
	κ_2	16.4413	γ_2	0.0292	μ_2	0.0482	K_{TT}^0	16.5191
	κ_3	-0.7566	γ_3	0.4075	μ_3	0.0878		
	κ_4	1.6437						

[†] Manual fit.

Note that the limiting damping parameter for $G_s = 100$ MPa has been fitted manually. Since the impedance for high values of G_s approaches the frequency dependent behaviour of the surface footings, the solution in Ibsen and Liingaard (2006a) is not valid. c^∞ for $G_s = 100$ MPa in Table 1.16 is in between the value for the suction caisson and a surface footing.

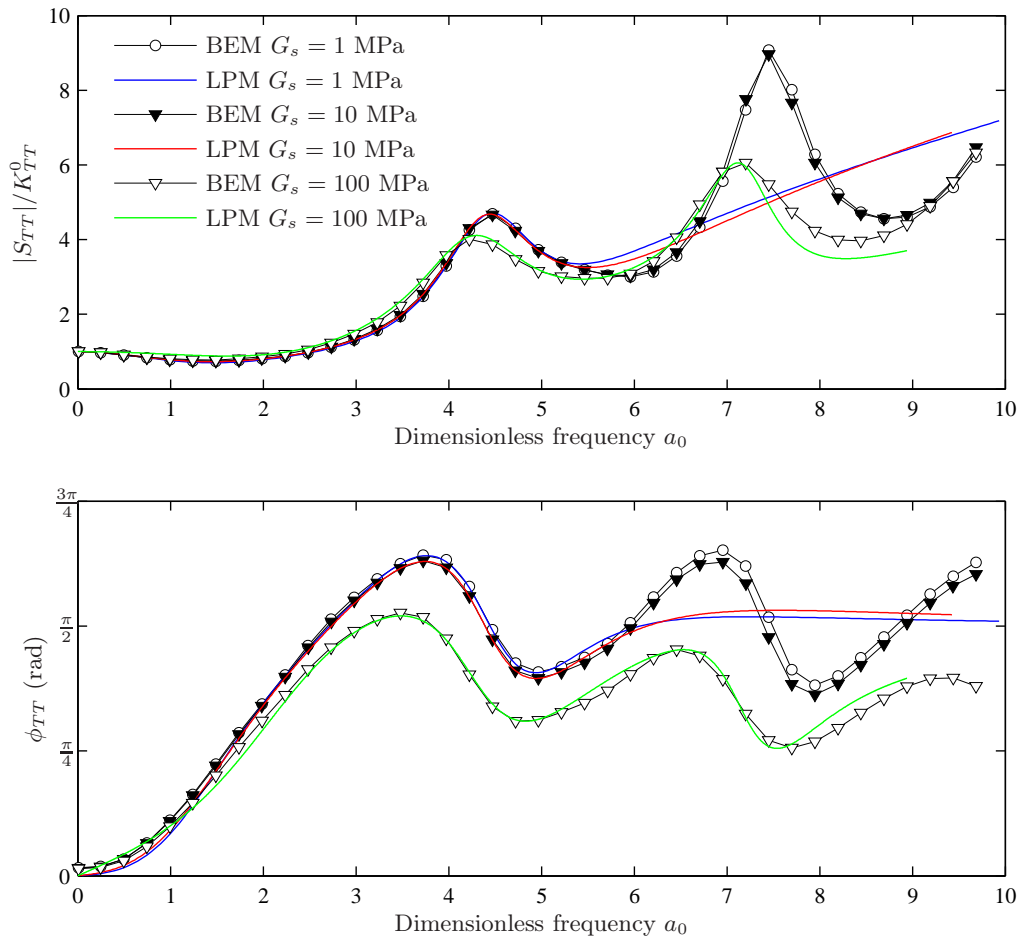


Figure 1.7: Torsional impedance: Boundary element solution and the corresponding lumped-parameter approximation. $\nu_s = 0.25$ and $\eta_s = 5\%$.

1.2 Assembly of the global dynamic stiffness matrix

The dynamic stiffness for each degree of freedom is given by three matrices \mathbf{K}_{dof} , \mathbf{C}_{dof} and \mathbf{M}_{dof} . The subscript 'dof' denotes the degree of freedom, which is either \mathbf{VV} , \mathbf{HH} , \mathbf{MM} , \mathbf{TT} or \mathbf{HM} . The matrices describing the dynamic stiffness for each of the degrees of freedom are denoted as local matrices in the following. Each local matrix contains frequency independent coefficients, which are determined by the procedure applied in the previous sections. The size of \mathbf{K}_{dof} , \mathbf{C}_{dof} and \mathbf{M}_{dof} are given by the numbers and types of discrete elements used to approximate the dynamic stiffness. The size of the local matrices are denoted by n_{dof} .

1.2.1 Structure of the local dynamic stiffness matrices

Each local matrix can be divided into four sections. The first section contain the stiffness, damping or mass coefficient of the external node of the lumped-parameter model, i.e the coefficient that enters the finite element formulation of the structural system. The second section contains the coefficients of the internal nodes of the lumped-parameter model, and finally, the third and fourth section contain coefficients that link the external and internal nodes. The structure of \mathbf{K}_{dof} , \mathbf{C}_{dof} and \mathbf{M}_{dof} are given as

$$\mathbf{K}_{\text{dof}} = \begin{bmatrix} \mathbf{k}_{\text{dof}}^{11} & \mathbf{k}_{\text{dof}}^{12} \\ \mathbf{k}_{\text{dof}}^{21} & \mathbf{k}_{\text{dof}}^{22} \end{bmatrix}, \quad \mathbf{C}_{\text{dof}} = \begin{bmatrix} \mathbf{c}_{\text{dof}}^{11} & \mathbf{c}_{\text{dof}}^{12} \\ \mathbf{c}_{\text{dof}}^{21} & \mathbf{c}_{\text{dof}}^{22} \end{bmatrix}, \quad \mathbf{M}_{\text{dof}} = \begin{bmatrix} \mathbf{m}_{\text{dof}}^{11} & \mathbf{m}_{\text{dof}}^{12} \\ \mathbf{m}_{\text{dof}}^{21} & \mathbf{m}_{\text{dof}}^{22} \end{bmatrix}. \quad (1.8)$$

The sub-matrices, denoted by the subscript ¹¹, contain only one component (1×1 matrices), The size of the sub-matrices denoted by the subscript ²² is $(n_{\text{dof}} - 1) \times (n_{\text{dof}} - 1)$, and the size of the sub-matrices denoted by the subscript ¹² and ²¹ are $1 \times (n_{\text{dof}} - 1)$ and $(n_{\text{dof}} - 1) \times 1$, respectively.

1.2.2 Structure of the global dynamic stiffness matrices

The dynamic stiffness relation for a generalized massless axisymmetric rigid foundation with six degrees of freedom (one vertical, two horizontal, two rocking and one torsional) is given in Ibsen and Liingaard (2006c). The stiffness formulation is given by a impedance matrix, $S_{ij}(a_0)$, relating the displacements and forces acting on the foundation. $S_{ij}(a_0)$ is a frequency dependent matrix with complex components, which does not fit into the framework of ordinary finite element codes. However, the lumped-parameter model represents a unbounded soil domain, and the soil-structure interaction of a massless foundation can be modelled by relatively few springs, dashpots and masses, all with real frequency-independent coefficients. Each degree of freedom at the foundation node of the structural model is coupled to a lumped-parameter model that may consist of additional internal degrees of freedom.

In this subsection the structure of the global dynamic stiffness matrices, based on the lumped-parameter models, will be explained. The global dynamic stiffness matrices are given for two- and three-dimensional problems.

Global dynamic stiffness matrices for 2D

A two-dimensional beam member is capable of axial deformation and ending in one principal plane. Each node in the finite element formulation is described by three degrees of freedom. For details, see Petyt (1998). The global matrices, \mathbf{K}^{2D} , \mathbf{C}^{2D} and \mathbf{M}^{2D} , representing the dynamic stiffness of a two-dimensional foundation are as follows

$$\mathbf{K}^{2D} = \begin{bmatrix} \mathbf{k}_{HH}^{11} & \mathbf{0} & \mathbf{k}_{HM}^{11} & \mathbf{k}_{HH}^{12} & \mathbf{0} & \mathbf{0} & \mathbf{k}_{HM}^{12} & \mathbf{0} \\ \mathbf{0} & \mathbf{k}_{VV}^{11} & \mathbf{0} & \mathbf{0} & \mathbf{k}_{VV}^{12} & \mathbf{0} & \mathbf{0} & \mathbf{0} \\ \mathbf{k}_{HM}^{11} & \mathbf{0} & \mathbf{k}_{MM}^{11} & \mathbf{0} & \mathbf{0} & \mathbf{k}_{MM}^{12} & \mathbf{0} & \mathbf{k}_{HM}^{12} \\ \hline \mathbf{k}_{HH}^{21} & \mathbf{0} & \mathbf{0} & \mathbf{k}_{HH}^{22} & \mathbf{0} & \mathbf{0} & \mathbf{0} & \mathbf{0} \\ \mathbf{0} & \mathbf{k}_{VV}^{21} & \mathbf{0} & \mathbf{0} & \mathbf{k}_{VV}^{22} & \mathbf{0} & \mathbf{0} & \mathbf{0} \\ \mathbf{0} & \mathbf{0} & \mathbf{k}_{MM}^{21} & \mathbf{0} & \mathbf{0} & \mathbf{k}_{MM}^{22} & \mathbf{0} & \mathbf{0} \\ \mathbf{0} & \mathbf{0} & \mathbf{k}_{HM}^{21} & \mathbf{0} & \mathbf{0} & \mathbf{0} & \mathbf{k}_{HM}^{22} & \mathbf{0} \\ \mathbf{k}_{HM}^{21} & \mathbf{0} & \mathbf{0} & \mathbf{0} & \mathbf{0} & \mathbf{0} & \mathbf{0} & \mathbf{k}_{HM}^{22} \end{bmatrix} \quad (1.9a)$$

$$\mathbf{C}^{2D} = \begin{bmatrix} \mathbf{c}_{HH}^{11} & \mathbf{0} & \mathbf{c}_{HM}^{11} & \mathbf{c}_{HH}^{12} & \mathbf{0} & \mathbf{0} & \mathbf{c}_{HM}^{12} & \mathbf{0} \\ \mathbf{0} & \mathbf{c}_{VV}^{11} & \mathbf{0} & \mathbf{0} & \mathbf{c}_{VV}^{12} & \mathbf{0} & \mathbf{0} & \mathbf{0} \\ \mathbf{c}_{HM}^{11} & \mathbf{0} & \mathbf{c}_{MM}^{11} & \mathbf{0} & \mathbf{0} & \mathbf{c}_{MM}^{12} & \mathbf{0} & \mathbf{c}_{HM}^{12} \\ \hline \mathbf{c}_{HH}^{21} & \mathbf{0} & \mathbf{0} & \mathbf{c}_{HH}^{22} & \mathbf{0} & \mathbf{0} & \mathbf{0} & \mathbf{0} \\ \mathbf{0} & \mathbf{c}_{VV}^{21} & \mathbf{0} & \mathbf{0} & \mathbf{c}_{VV}^{22} & \mathbf{0} & \mathbf{0} & \mathbf{0} \\ \mathbf{0} & \mathbf{0} & \mathbf{c}_{MM}^{21} & \mathbf{0} & \mathbf{0} & \mathbf{c}_{MM}^{22} & \mathbf{0} & \mathbf{0} \\ \mathbf{0} & \mathbf{0} & \mathbf{c}_{HM}^{21} & \mathbf{0} & \mathbf{0} & \mathbf{0} & \mathbf{c}_{HM}^{22} & \mathbf{0} \\ \mathbf{c}_{HM}^{21} & \mathbf{0} & \mathbf{0} & \mathbf{0} & \mathbf{0} & \mathbf{0} & \mathbf{0} & \mathbf{c}_{HM}^{22} \end{bmatrix} \quad (1.9b)$$

$$\mathbf{M}^{2D} = \begin{bmatrix} \mathbf{m}_{HH}^{11} & \mathbf{0} & \mathbf{m}_{HM}^{11} & \mathbf{m}_{HH}^{12} & \mathbf{0} & \mathbf{0} & \mathbf{m}_{HM}^{12} & \mathbf{0} \\ \mathbf{0} & \mathbf{m}_{VV}^{11} & \mathbf{0} & \mathbf{0} & \mathbf{m}_{VV}^{12} & \mathbf{0} & \mathbf{0} & \mathbf{0} \\ \mathbf{m}_{HM}^{11} & \mathbf{0} & \mathbf{m}_{MM}^{11} & \mathbf{0} & \mathbf{0} & \mathbf{m}_{MM}^{12} & \mathbf{0} & \mathbf{m}_{HM}^{12} \\ \hline \mathbf{m}_{HH}^{21} & \mathbf{0} & \mathbf{0} & \mathbf{m}_{HH}^{22} & \mathbf{0} & \mathbf{0} & \mathbf{0} & \mathbf{0} \\ \mathbf{0} & \mathbf{m}_{VV}^{21} & \mathbf{0} & \mathbf{0} & \mathbf{m}_{VV}^{22} & \mathbf{0} & \mathbf{0} & \mathbf{0} \\ \mathbf{0} & \mathbf{0} & \mathbf{m}_{MM}^{21} & \mathbf{0} & \mathbf{0} & \mathbf{m}_{MM}^{22} & \mathbf{0} & \mathbf{0} \\ \mathbf{0} & \mathbf{0} & \mathbf{m}_{HM}^{21} & \mathbf{0} & \mathbf{0} & \mathbf{0} & \mathbf{m}_{HM}^{22} & \mathbf{0} \\ \mathbf{m}_{HM}^{21} & \mathbf{0} & \mathbf{0} & \mathbf{0} & \mathbf{0} & \mathbf{0} & \mathbf{0} & \mathbf{m}_{HM}^{22} \end{bmatrix} \quad (1.9c)$$

The upper left part of the matrices are to be added to the foundation node of the structural finite element model. The remaining components of the matrices correspond to the additional internal degrees of freedom, arising from the lumped-parameter models. The number of additional degrees of freedom for the two-dimensional model is $(n_{VV} - 1) + (n_{HH} - 1) + (n_{MM} - 1) + 2(n_{HM} - 1)$, i.e. the sum of the additional internal degrees of freedom.

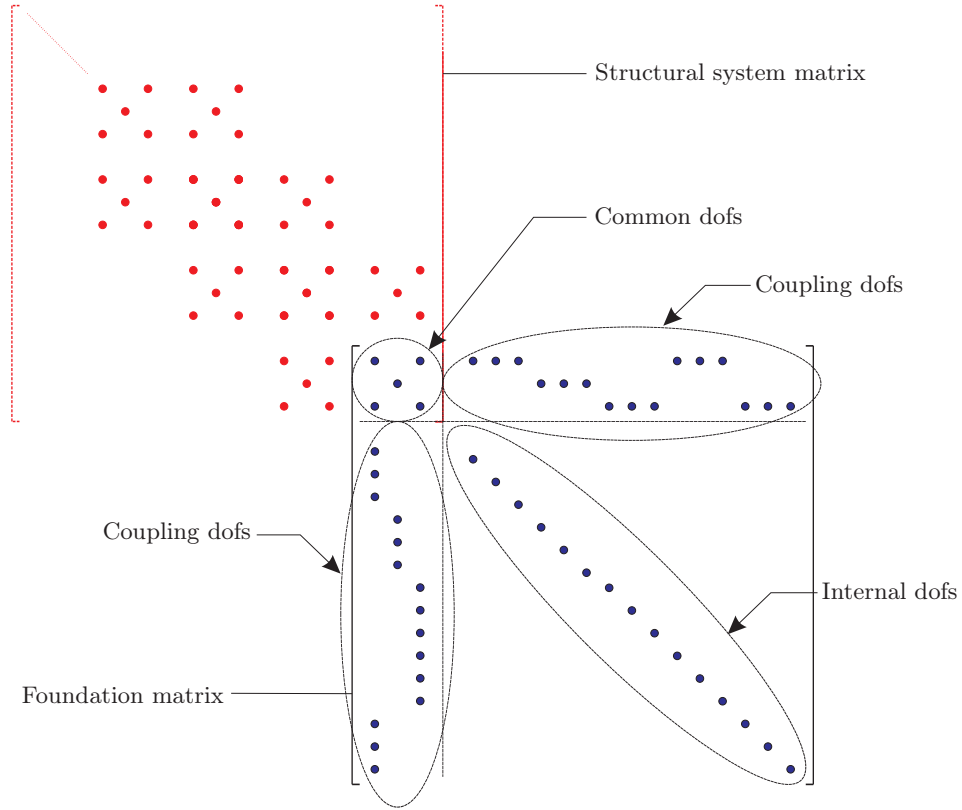


Figure 1.8: Assembly between global foundation matrices and the structural system.

The assembly between the global matrices of the foundation and the system matrices of the structural system is sketched in Figure 1.8.

Global dynamic stiffness matrices for 3D

A three-dimensional beam member is capable of axial deformation, bending in two principal planes and torsion about the beam axis. Each node in the finite element formulation is described by six degrees of freedom. For details, see Petyt (1998). The global matrices, \mathbf{K}^{3D} , \mathbf{C}^{3D} and \mathbf{M}^{3D} , representing the dynamic stiffness of a three-dimensional foundation are as follows:

$$\mathbf{K}^{3D} = \begin{bmatrix} \bar{\mathbf{k}}^{11} & \bar{\mathbf{k}}^{12} \\ \bar{\mathbf{k}}^{21} & \bar{\mathbf{k}}^{22} \end{bmatrix}, \mathbf{C}^{3D} = \begin{bmatrix} \bar{\mathbf{c}}^{11} & \bar{\mathbf{c}}^{12} \\ \bar{\mathbf{c}}^{21} & \bar{\mathbf{c}}^{22} \end{bmatrix}, \mathbf{M}^{3D} = \begin{bmatrix} \bar{\mathbf{m}}^{11} & \bar{\mathbf{m}}^{12} \\ \bar{\mathbf{m}}^{21} & \bar{\mathbf{m}}^{22} \end{bmatrix} \quad (1.10)$$

where $\bar{\mathbf{k}}^{11}$, $\bar{\mathbf{k}}^{12}$, $\bar{\mathbf{k}}^{21}$ and $\bar{\mathbf{k}}^{22}$ are given as

$$\bar{\mathbf{k}}^{11} = \begin{bmatrix} k_{VV}^{11} & 0 & 0 & 0 & 0 & 0 \\ 0 & k_{HH}^{11} & 0 & 0 & 0 & -k_{HM}^{11} \\ 0 & 0 & k_{HH}^{11} & 0 & k_{HM}^{11} & 0 \\ 0 & 0 & 0 & k_{TT}^{11} & 0 & 0 \\ 0 & 0 & k_{HM}^{11} & 0 & k_{MM}^{11} & 0 \\ 0 & -k_{HM}^{11} & 0 & 0 & 0 & k_{MM}^{11} \end{bmatrix} \quad (1.11a)$$

$$\bar{\mathbf{k}}^{12} = \begin{bmatrix} k_{VV}^{12} & 0 & 0 & 0 & 0 & 0 & 0 & 0 & 0 & 0 \\ 0 & k_{HH}^{12} & 0 & 0 & 0 & 0 & -k_{HM}^{12} & 0 & 0 & 0 \\ 0 & 0 & k_{HH}^{12} & 0 & 0 & 0 & 0 & k_{HM}^{12} & 0 & 0 \\ 0 & 0 & 0 & k_{TT}^{12} & 0 & 0 & 0 & 0 & 0 & 0 \\ 0 & 0 & 0 & 0 & k_{MM}^{12} & 0 & 0 & 0 & k_{HM}^{12} & 0 \\ 0 & 0 & 0 & 0 & 0 & k_{MM}^{12} & 0 & 0 & 0 & -k_{HM}^{12} \end{bmatrix} \quad (1.11b)$$

$$\bar{\mathbf{k}}^{21} = \begin{bmatrix} k_{VV}^{21} & 0 & 0 & 0 & 0 & 0 \\ 0 & k_{HH}^{21} & 0 & 0 & 0 & 0 \\ 0 & 0 & k_{HH}^{21} & 0 & 0 & 0 \\ 0 & 0 & 0 & k_{TT}^{21} & 0 & 0 \\ 0 & 0 & 0 & 0 & k_{MM}^{21} & 0 \\ 0 & 0 & 0 & 0 & 0 & k_{MM}^{21} \\ 0 & 0 & 0 & 0 & 0 & -k_{HM}^{21} \\ 0 & 0 & 0 & 0 & k_{HM}^{21} & 0 \\ 0 & 0 & k_{HM}^{21} & 0 & 0 & 0 \\ 0 & -k_{HM}^{21} & 0 & 0 & 0 & 0 \end{bmatrix} \quad (1.11c)$$

$$\bar{\mathbf{k}}^{22} = \begin{bmatrix} k_{VV}^{22} & 0 & 0 & 0 & 0 & 0 & 0 & 0 & 0 & 0 \\ 0 & k_{HH}^{22} & 0 & 0 & 0 & 0 & 0 & 0 & 0 & 0 \\ 0 & 0 & k_{HH}^{22} & 0 & 0 & 0 & 0 & 0 & 0 & 0 \\ 0 & 0 & 0 & k_{TT}^{22} & 0 & 0 & 0 & 0 & 0 & 0 \\ 0 & 0 & 0 & 0 & k_{MM}^{22} & 0 & 0 & 0 & 0 & 0 \\ 0 & 0 & 0 & 0 & 0 & k_{MM}^{22} & 0 & 0 & 0 & 0 \\ 0 & 0 & 0 & 0 & 0 & 0 & -k_{HM}^{22} & 0 & 0 & 0 \\ 0 & 0 & 0 & 0 & 0 & 0 & 0 & k_{HM}^{22} & 0 & 0 \\ 0 & 0 & 0 & 0 & 0 & 0 & 0 & 0 & k_{HM}^{22} & 0 \\ 0 & 0 & 0 & 0 & 0 & 0 & 0 & 0 & 0 & -k_{HM}^{22} \end{bmatrix} \quad (1.11d)$$

The sub-matrices in \mathbf{C}^{3D} and \mathbf{M}^{3D} are similar to those for \mathbf{K}^{3D} , given by the equations in 1.11. The sub-matrices are obtained by replacing \mathbf{k} by \mathbf{c} and \mathbf{m} , respectively. The number of additional degrees of freedom for the three-dimensional model is $(n_{VV} - 1) + 2(n_{HH} - 1) + (n_{TT} - 1) + 2(n_{MM} - 1) + 4(n_{HM} - 1)$. Note that the rows in $\bar{\mathbf{k}}^{11}$ (and hence $\bar{\mathbf{c}}^{11}$ and $\bar{\mathbf{m}}^{11}$) can be interchanged, depending on the arrangement of the degrees

of freedom in the structural finite element formulation. Appropriate rearrangement of the remaining sub-matrices ($\bar{\mathbf{k}}^{12}$, $\bar{\mathbf{k}}^{21}$ and $\bar{\mathbf{k}}^{22}$) should then be performed as well.

1.3 Direct analysis of the steady state response for lumped-parameter models

The steady state response is determined by solving the equation of motion for a harmonic response, given by

$$\mathbf{M}\ddot{\mathbf{u}} + \mathbf{C}\dot{\mathbf{u}} + \mathbf{K}\mathbf{u} = \mathbf{f}e^{i\omega t}, \quad (1.12)$$

where \mathbf{M} , \mathbf{C} and \mathbf{K} are the mass, damping and stiffness matrices of the vibrating structure, respectively. \mathbf{M} , \mathbf{C} and \mathbf{K} are assembled from the global matrices of the foundation and the system matrices of the structural system, as sketched in Figure 1.9. \mathbf{u} is a column vector containing the nodal displacements and \mathbf{f} is a column vector of nodal forces. t is time and i is the imaginary unit, $i = \sqrt{-1}$. The equation of motion in Equation 1.12 is solved by direct analysis (Petyt 1998). The solution to Equation 1.12 is then

$$\mathbf{u} = [\mathbf{K} - \omega^2\mathbf{M} + i\omega\mathbf{C}]^{-1} \mathbf{f}e^{i\omega t} \quad (1.13)$$

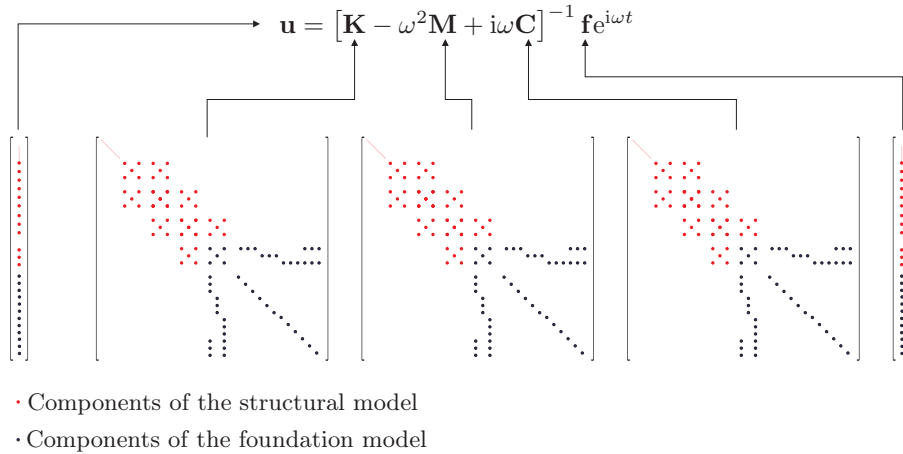


Figure 1.9: Structure of the matrices and vectors for the direct analysis.

Bibliography

- Andersen, L. and C. Jones (2001). BEASTS — A Computer Program for Boundary Element Analysis of Soil and Three-dimensional Structures. ISVR Technical Memorandum 868, Institute of Sound and Vibration Research, University of Southampton.
- Ibsen, L. B. and M. Liingaard (2006a). Dynamic stiffness of suction caissons—torsion, sliding and rocking. DCE Technical report 8, Department of Civil Engineering, Aalborg University.
- Ibsen, L. B. and M. Liingaard (2006b). Dynamic stiffness of suction caissons—vertical vibrations. DCE Technical report 7, Department of Civil Engineering, Aalborg University.
- Ibsen, L. B. and M. Liingaard (2006c). Lumped-parameter models. DCE Technical report 11, Department of Civil Engineering, Aalborg University.
- Petyt, M. (1998). *Introduction to Finite Element Vibration Analysis*. Cambridge: Cambridge University Press.